# Altering the Specificity of Restriction Endonuclease: Effect of Replacing $Mg^{2+}$ with $Mn^{2+}$ †

Ming-ta Hsu*,‡ and Paul Berg

ABSTRACT: In the presence of 100 mM Tris buffer (pH 7.5) and 1–10 mM $Mg^{2+}$ *Eco*RI endonuclease cleaves DNA at a specific nucleotide sequence and in a characteristic way: -G↓AATTC-. But if $Mg^{2+}$ is replaced by $Mn^{2+}$, the specificity of the cleavage is relaxed and cleavages occur at many other sites; moreover, there appears to be a hierarchy of cleavage rates at the pseudo-*Eco*RI restriction sites. For example, SV40 DNA is cleaved only once in the usual digestion conditions, but with $Mn^{2+}$ more than ten cleavages are made; the five most rapidly cleaved SV40 DNA map locations are $0/1.0 > 0.93 > 0.33 \cong 0.42 > 0.29 \cong 0.49 > 0.25$. $Mn^{2+}$ also alters the restriction specificity of *Hin*dIII but not *Hpa*II endonuclease.

Restriction endonucleases cleave double-stranded DNA at specific nucleotide sequences generating a characteristic assortment of fragments (Arber, 1974). Generally, but not always, the oligonucleotide sequence at which the cleavage occurs has a twofold axis of symmetry; i.e., the sequence is the same in each strand taking into account the polarity of the two chains (Arber, 1974). Some enzymes, but not all, produce staggered cleavages in the two strands, thereby generating fragments with single-stranded termini that are identical and complementary to each other, so-called, cohesive termini. Consequently, restriction endonucleases have become extremely valuable reagents for dissecting a variety of DNA genomes and for analyzing the structure and organization of their genetic elements; they are also central to attempts to construct recombinant DNAs in vitro.

An important property of restriction endonucleases is their specificity for the nucleotide sequences they cleave. In using *Eco*RI endonuclease we noted that the enzyme made many more cleavages in SV40 DNA when $Mn^{2+}$ was used in place of $Mg^{2+}$ in the reaction. In this paper we report on the nature and location of the cleavages in SV40 DNA catalyzed by *Eco*RI endonuclease in the presence of $Mn^{2+}$ (the *Eco*RI-Mn reaction), as well as the effect of $Mn^{2+}$ on the specificity of *Hpa*II and *Hin*dIII endonucleases. While this work was in progress Polisky et al. (1975) reported that *Eco*RI endonuclease cleaves DNA at sites other than *Eco*RI restriction sequences when the ionic strength is lowered and the pH exceeds 8; these have been referred to as *Eco*RI* endonuclease cleavages.

## Materials and Methods

(A) *SV40 DNA.* SV40 DNA was purified from CV1 cells infected with a plaque purified isolate of SVS (Takemoto et al., 1966) at low multiplicity (0.1 pfu/cell). Viral DNA was obtained by Hirt's procedure (Hirt, 1967) followed by phenol and chloroform extractions, and CsCl–ethidium bromide equilibrium centrifugation (Radloff et al., 1967). Ethidium bromide was removed from the DNA by passage over Dowex-50 and extensive dialysis.

(B) *Restriction Endonucleases. Eco*RI endonuclease was prepared by a modification of the Greene et al. procedure (1974). Bacterial cells, suspended (0.2 g/mL) in a solution containing 10% sucrose, 0.2 M $(NH_4)_2SO_4$, 0.05 M Tris (pH 7.5), and 10 mM spermidine, were homogenized in a blender by three 30-s bursts with 30-s pauses and, after incubation for 30 min at 0 °C with lysozyme (0.1 mg/mL), the lysate was centrifuged at 20 000 rpm for 60 min at 0 °C. Ammonium sulfate was added to the supernatant (35 g/100 mL) and, after 20 min of stirring, the mixture was centrifuged at 18 000 rpm for 10 min. The pellet was extracted sequentially with 50-mL aliquots of 47.5%, 45%, 42.5%, and 40% saturated ammonium sulfate solution in EB buffer (10 mM $K_2HPO_4$, pH 7.0, 1 mM EDTA, 7 mM mercaptoethanol) and then with 20 mL of 37.5%, 35%, 32.5%, 30% saturated $(NH_4)_2SO_4$ solution in EB buffer. The 30–40% ammonium sulfate extracts, which contain the major *Eco*RI endonuclease activity, were pooled, and the protein was precipitated by adding ammonium sulfate to 65% saturation. The pellet was resuspended in and dialyzed against EB buffer before loading on the phosphocellulose column (Greene et al., 1974). *Eco*RI endonuclease was eluted from the column by a linear NaCl gradient 0.35 M to 0.7 M in EB buffer. One unit of *Eco*RI endonuclease activity is the amount of enzyme needed to cleave 40 μg of SV40 DNA in 30 min at 37 °C. The enzyme was then dialyzed against 10 mM Tris (pH 7.0), 0.2% NP40, and 0.2 M NaCl.

Purified *Eco*RI endonuclease was also given to us by R. W. Davis (Stanford University), P. Modrich (1976), and R. Roberts (Cold Spring Harbor Laboratory).

*Hin*dIII (Smith and Wilcox, 1970) and *Hpa*I and *Hpa*II (Sharp et al., 1973) endonucleases were purified according to published procedures. The conditions for various enzyme digestions are given in the legends to the figures.

(C) *Gel Electrophoresis.* Agarose gels, 1.2% or 2.5% (13 cm × 6 mm), were used to analyze the pattern and sizes of DNA fragments generated by enzyme digestion. Electrophoresis was carried out at pH 7.9 in a buffer containing Tris (10.8 g/L), boric acid (5.5 g/L), and EDTA (0.93 g/L) at 40 V until the bromophenol blue dye reached the end of the gel.

DNA in the gels was stained with ethidium bromide solution (0.5 μg/mL) for 20 min and the fluorescent bands, induced with short wavelength UV light, were recorded on Polaroid film No. 105.

† From the Department of Biochemistry, Stanford University Medical Center, Stanford, California 94305. *Received April 29, 1977; revised manuscript received October 7, 1977.* This work was supported by a research grant to Paul Berg from the U.S. Public Health Service, GM 13235-12, and the American Cancer Society, VC-23F; Ming-ta Hsu was a Research Fellow of the Leukemia Society of America.

‡ Present address: The Rockefeller University, Department of Molecular and Cell Biology, New York, N.Y. 10021.

0006-2960/78/0417-0131$01.00/0 

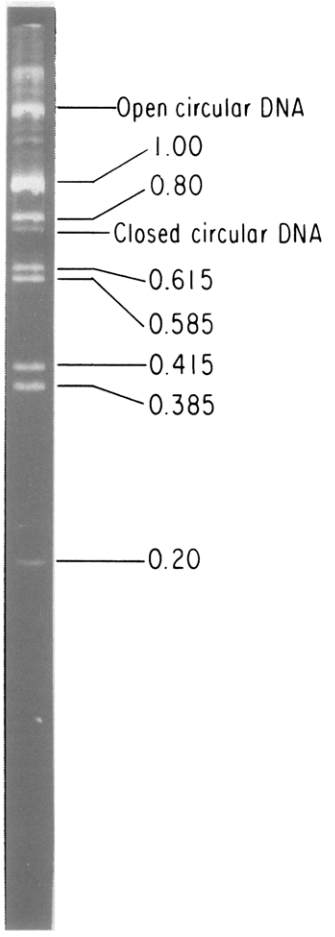


FIGURE 1: DNA fragments of known length used as standards for estimating the sizes of the restriction endonuclease digest products. They consist of (i) full length linear SV40 DNA obtained by digesting SV40 circular DNA with *Eco*RI endonuclease under standard conditions and (ii) the partial digest of SV40 DNA with *Hpa*I endonuclease to yield both partial and limit digest products. SV40 relaxed and supercoiled circular DNAs are also included.

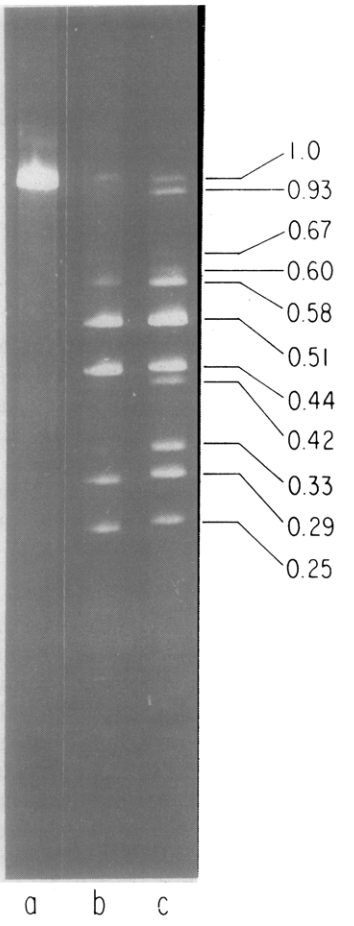


FIGURE 3: Effect of $Mn^{2+}$ on *Eco*RI endonuclease digestion of SV40 DNA. SV40 DNA, 0.2 μg, was digested with 2 units of *Eco*RI endonuclease in 100 mM Tris, pH 7.5, for 30 min at 37 °C with (a) 10 mM $Mg^{2+}$; (b) 2 mM $Mn^{2+}$; (c) 2 mM $Mn^{2+}$ plus 2 mM $Mg^{2+}$. The size of the DNA fragments was determined by coelectrophoresis of the sample with the length standards shown in Figure 1.

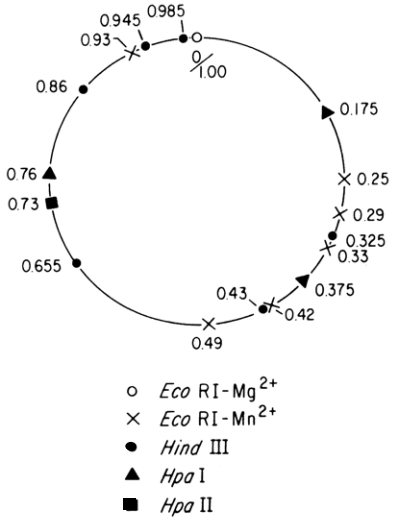


Restriction Endo Nuclease-cleavage Sites in SV40 DNA

FIGURE 2: Sites of cleavage of SV40 DNA by several restriction endonucleases. Maps of coordinates are expressed as SV40 fractional lengths from the *Eco*RI-$Mg^{2+}$ cleavage site designated 0/1.0.

The molecular lengths of DNA fragments were determined from their electrophoretic mobility in agarose gels using SV40 DNA fragments of known lengths as standards. The electrophoretic patterns of the DNA length standards are shown in Figure 1.

## Results

(A) *Replacing $Mg^{2+}$ by $Mn^{2+}$ in the EcoRI endonuclease reaction* changes the specificity of the cleavages in DNA (Figure 2).

*Eco*RI endonuclease cleaves SV40 DNA to a unique full length linear DNA in 100 mM Tris buffer (pH 7.5) containing 10 mM $Mg^{2+}$ (Morrow and Berg, 1973; Mulder and Delius, 1973) (Figure 3, track a). When 2 mM $Mn^{2+}$ replaces the $Mg^{2+}$ or is added in addition to the $Mg^{2+}$, the DNA is cleaved to an assortment of fragments with discrete sizes (Figure 3, tracks b and c). The digestion pattern was similar using the reaction conditions described by Poliskey et al. (1975) but the rate of cleavage was slower (data not shown). This result is not unique to SV40 DNA as the same phenomenon occurs with λ phage DNA (Figure 4, tracks c and d) and adenovirus 2 DNA (data not shown). Even if the λ DNA carries the *Eco*RI modification and is resistant to cleavage with *Eco*RI endonuclease with $Mg^{2+}$, extensive cleavage still occurs with $Mn^{2+}$ (Figure 4, tracks a and b).

The accumulation of discrete size fragments at all stages in the incubation argues against nonspecific endonuclease action;

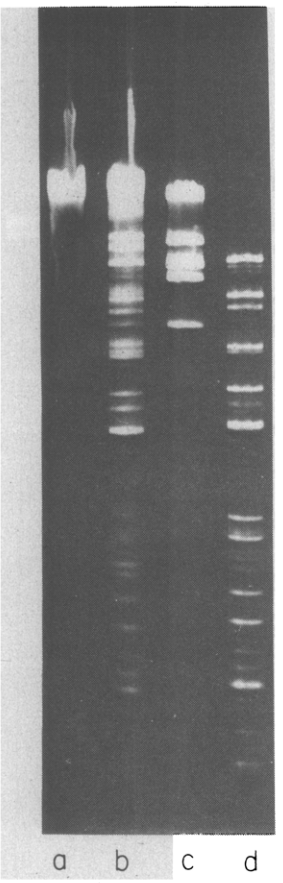


FIGURE 4: Effect of $Mn^{2+}$ on *Eco*RI endonuclease digestion of λ and *Eco*RI-modified λ DNA; 0.6 μg of *Eco*RI-modified (a and b) or unmodified DNA (c and d) was digested with *Eco*RI endonuclease at 37 °C for 30 min in 100 mM Tris with 10 mM $Mg^{2+}$ (a and c) or 2 mM $Mn^{2+}$ (b and d).

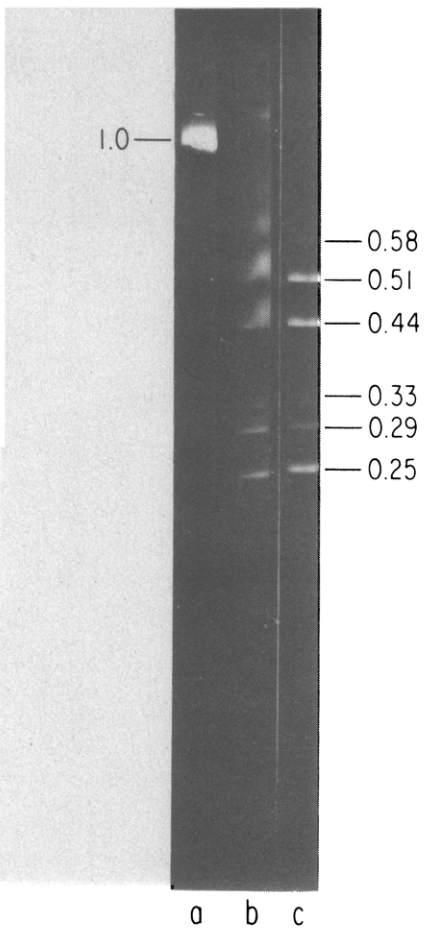


FIGURE 5: Effect of $Mn^{2+}$ on the digestion of SV40 DNA with highly purified *Eco*RI endonuclease described by P. Modrich (Modrich and Zabel, 1976). SV40 DNA (0.5 μg) was digested with 1 unit of *Eco*RI endonuclease for 30 min at 37 °C in 100 mM Tris (pH 7.5) with 10 mM $Mg^{2+}$ (track a) or with 2 mM $Mn^{2+}$ (track b). SV40 DNA digested with our preparation of *Eco*RI endonuclease is shown in track c for comparison.

moreover, three highly purified *Eco*RI endonuclease preparations obtained from R. Roberts, R. W. Davis, and P. Modrich (Modrich and Zabel, 1976), the latter two of which have been judged by these investigators to be homogeneous using several physical criteria, cause the same $Mn^{2+}$-induced multiple cleavages of SV40 DNA (Figure 5). Supporting the view that these new cleavages are catalyzed by *Eco*RI endonuclease per se is the finding that about 50% of the DNA fragments generated after 20 min in the *Eco*RI-$Mn^{2+}$ reaction are converted to covalently closed circular DNA during incubation with DNA ligase for 5 days at 10 °C (Mertz and Davis, 1972). This finding indicates that the cleavages occurring at "pseudo-*Eco*RI" sites also generate cohesive ends.

Studies of the kinetics of the *Eco*RI-$Mn^{2+}$ reaction revealed a progression in the appearance of the different fragments (Figure 6). Early in the reaction larger fragments predominate, many of which disappear and are replaced by smaller fragments later in the reaction; in a limit digest the average size of the fragments is less than 0.10 SV40 fractional length. This behavior indicates the existence of a hierarchy in the sensitivity of the various sites to cleavage by *Eco*RI-$Mn^{2+}$.

(B) *Mapping the Sites Cleaved in the EcoRI-Mn$^{2+}$ Reaction.* Cleavage of SV40 DNA with *Eco*RI-$Mn^{2+}$ seems to occur most readily at the already known *Eco*RI endonuclease restriction site at map position 0/1.0 (Morrow and Berg, 1973; Mulder and Delius, 1973). Virtually the same fragmentation pattern is produced from covalently closed circular and *Eco*RI endonuclease generated (in $Mg^{2+}$) linear SV40 DNA (compare tracks a and b in Figure 6 with tracks a and b in Figure 7). Moreover, when *Eco*RI-$Mn^{2+}$ mediated cleavages are made in linear DNA molecules whose ends correspond to map coordinate 0.735 (those produced by *Hpa*II endonuclease (Sharp et al., 1973)), the most prominent early products are fragments of 0.73 and 0.27 SV40 fractional length (Figure 8, track a). Polisky et al. (1975) also concluded that *Eco*RI* endonuclease cleaved the true *Eco*RI sites preferentially.

The next most frequent cleavages by *Eco*RI-$Mn^{2+}$ occur at three sites on the SV40 DNA map: 0.93, 0.42, and 0.33 (see Figure 2). These were deduced as follows.

(i) Amongst the earliest products appearing in the *Eco*RI-$Mn^{2+}$ digest is a fragment 0.93 SV40 fractional length (Figure 6, but more clearly in Figure 7). This could arise from a cleavage of the *Eco*RI endonuclease generated linear DNA at map coordinate 0.93 or 0.07. But because a prominent early product in the *Eco*RI-$Mn^{2+}$ digest of *Hpa*II endonuclease generated linear DNA is a 0.20 SV40 fractional length fragment, and no 0.67 SV40 fractional length fragment has been seen even transiently (Figure 8), the most likely cleavage site is at map coordinate 0.93 (see Figure 2).

When the SV40 DNA fragment from coordinate 0.83 to 1.00 generated by *Eco*RI and *Hha*I endonucleases digestion of SV40 DNA is digested with *Eco*RI-$Mn^{2+}$ under conditions similar to those presented in Figure 8b, two fragments of 0.10 and 0.07 SV40 fractional length are produced; no cleavage of this fragment occurred when $Mg^{2+}$ was used in the incubation

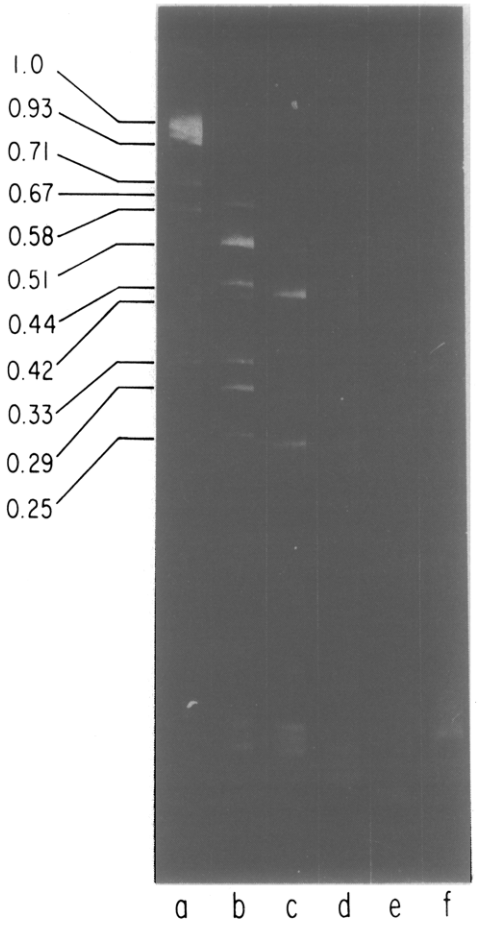


FIGURE 6: Kinetics of SV40 DNA digestion of *Eco*RI endonuclease with $Mn^{2+}$. SV40 DNA (0.2 μg) was digested with 2 units of *Eco*RI endonuclease in 100 mM Tris buffer (pH 7.5) with 1 mM $Mn^{2+}$ at 37 °C for (a) 5 min, (b) 30 min, (c) 1 h, (d) 4 h, (e) 6 h, (f) overnight (12 h).

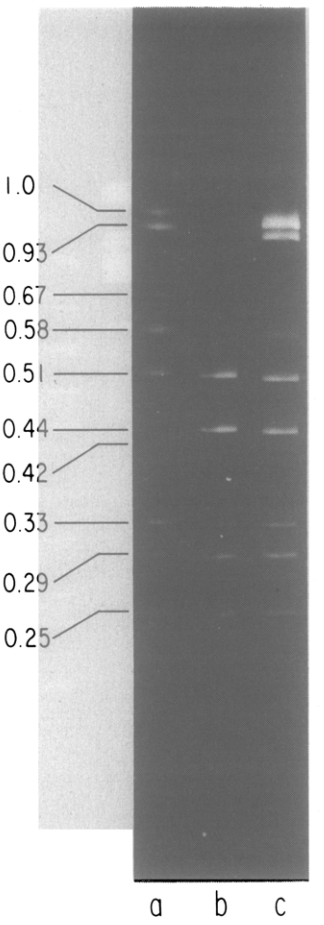


FIGURE 7: Effect of $Mn^{2+}$ on the *Eco*RI endonuclease digestion of *Eco*RI endonuclease-generated linear SV40 DNA. *Eco*RI endonuclease-generated linear SV40 DNA (0.2 μg) was digested with 2 units of *Eco*RI endonuclease in 100 mM Tris (pH 7.5) with 2 mM $Mn^{2+}$ at 37 °C for (a) 4 min, (b) 30 min, (c) sample in b plus SV40 form I DNA digested with *Eco*RI endonuclease in the presence of $Mn^{2+}$.

(data not shown). This confirms that there is an *Eco*RI-$Mn^{2+}$ cleavage site at coordinate 0.93.

(ii) DNA fragments of 0.67, 0.58, 0.42, and 0.33 SV40 fractional length are also prominent early products in the *Eco*RI-$Mn^{2+}$ digestion of SV40 DNA (track a in Figures 6 and 7). The 0.67 and 0.33 fragments as well as the 0.58 and 0.42 fragments are very likely pairs resulting from single cleavages of full length linear DNA. The coordinates of these two cleavages, which could be at any two of the map positions mentioned above, can be deduced by examining the early products of the digestion of *Hpa*II endonuclease generated linear DNA (Figure 8). Assuming that this full length DNA molecule is very rapidly reduced to one of 0.73 SV40 fractional length by a cleavage at the "true" *Eco*RI restriction site (map position 0/1.0), subsequent single hits should yield pairs of fragments whose molecular size adds up to 0.73 SV40 fractional length. Figure 8 shows that, amongst the earliest products produced in this digest, there are four fragments that are candidates for such pairs, e.g., 0.42 plus 0.32, and 0.40 plus 0.33. Their origin is most readily explained if cleavage occurs relatively rapidly at SV40 map positions 0.33 and 0.42.

(iii) The existence of *Eco*RI-$Mn^{2+}$ cleavage sites at SV40 map coordinates 0.33 and 0.42 predicts that fragments of 0.60 and 0.51 should also be found early in the reaction; these can arise from cleavages at map positions 0.33 and 0.93 or 0.42 and 0.93. The 0.51 SV40 fractional length fragment appears early and persists throughout, but the 0.60 fragment occurs only transiently, probably because it is converted to the 0.51 fragment by a cleavage at map position 0.42.

The data presented above shows that in the presence of $Mn^{2+}$ *Eco*RI endonuclease can cleave SV40 DNA at map coordinates 0.93, 0.33, and 0.42 as well as at the "true" *Eco*RI restriction site at map position 0/1.0.

Other sites are also cleaved in the *Eco*RI-$Mn^{2+}$ reaction, although at a slower rate. Three sites at which *Eco*RI-$Mn^{2+}$ cleaves SV40 DNA slowly are at map coordinates 0.25, 0.29, and 0.49; they were identified from the fragment patterns shown in Figures 6 and 7 and arguments analogous to those discussed above.

(i) Figure 6 shows that progressive digestion of SV40 DNA with *Eco*RI-$Mn^{2+}$ yields a fragment of 0.25 SV40 fractional length; this occurs regardless of whether the DNA substrate is circular or *Eco*RI or *Hpa*II endonuclease generated linear DNAs (see Figures 7 and 8). This suggests a cleavage site at map coordinate 0.25; the other fragment produced by the same cleavage cannot be detected because it is further degraded. As will be discussed in section D, at high levels of ethidium bromide SV40 DNA is cleaved by *Eco*RI-$Mn^{2+}$ only at map positions 0/1.0 and 0.25. This confirms the existence of an *Eco*RI-$Mn^{2+}$ cleavage site at map coordinate 0.25.

(ii) A fragment 0.29 SV40 fractional length appears transiently during the *Eco*RI-$Mn^{2+}$ cleavage of SV40 DNA (Figure 6). This could be explained by a cleavage at map position 0.29 or 0.71. If the cleavage had occurred at 0.71, fragments of 0.22 (0.71 to 0.93) should have appeared in the digestion of circular or *Eco*RI endonuclease generated linear

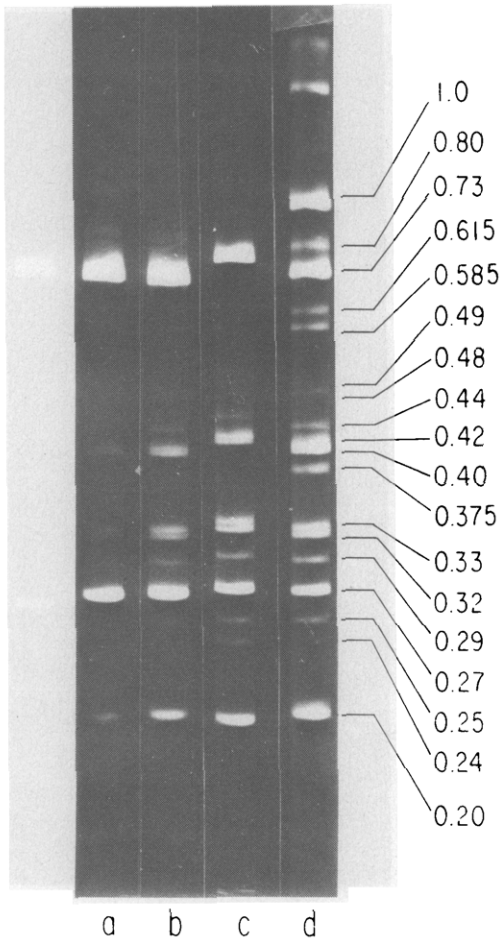


FIGURE 8: Digestion of *Hpa*II endonuclease generated linear SV40 DNA with *Eco*RI endonuclease in the presence of $Mn^{2+}$. SV40 *Hpa*II endonuclease generated linear DNA (0.4 $\mu$g) was digested with 2 units of *Eco*RI endonuclease in 100 mM Tris (pH 7.5) and 2 mM $Mn^{2+}$ at 37 °C for (a) 5 min, (b) 15 min, (c) 30 min, (d) sample c plus length standards.

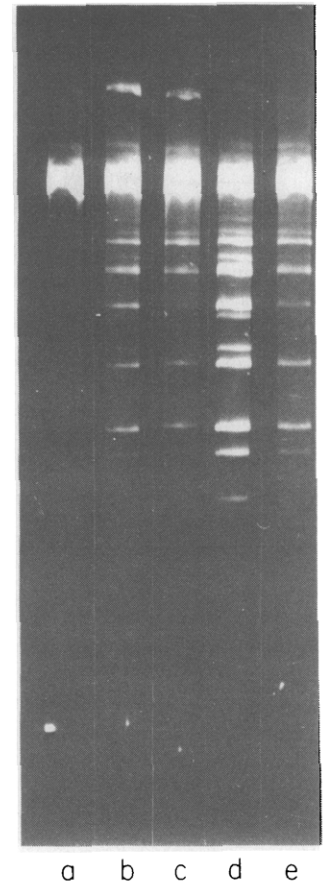


FIGURE 9: Effect of salt on the digestion of SV40 DNA by *Eco*RI endonuclease in the presence of $Mn^{2+}$. SV40 form I DNA (0.8 $\mu$g) was digested with 2 units of *Eco*RI endonuclease in (a) 200 mM Tris (pH 7.5) for 5 min at 37 °C, (b) 100 mM Tris (pH 7.5) for 5 min at 37 °C, (c) 100 mM Tris (pH 7.5), 50 mM NaCl for 5 min at 37 °C, (d) same as b but for 15 min, (e) same as c except for 15 min.

DNA. Since a 0.22 fragment was not detected, we surmise that the cleavage occurred at map position 0.29 and that the 0.71 fractional length fragment is not detected because of the strong likelihood that cleavages already had occurred at map positions 0.33 and 0.42.

(iii) During the digestion of SV40 DNA with *Eco*RI-$Mn^{2+}$, a fragment of 0.44 SV40 fractional length accumulates (Figures 6 and 7). This can be explained by rapid cleavages at map positions 0/1.0 and 0.93 followed by a slower cleavage at 0.49, an interpretation which is consistent with the relatively slow appearance of a 0.24 SV40 fractional length fragment during the digestion of the *Hap*II endonuclease generated linear DNA (Figure 8). Further support for this assignment comes from the finding that a 0.38 SV40 fractional length fragment from the region bounded by map coordinates 0.38 to 0.76 (the *Hpa*IC fragment produced by *Hpa*I endonuclease digestion of SV40 DNA (Sharp et al., 1973)) yields a 0.27 SV40 fractional length fragment after digestion with *Eco*RI-$Mn^{2+}$ (data not shown).

Taken together our data show that with $Mn^{2+}$ instead of $Mg^{2+}$, *Eco*RI endonuclease cleaves SV40 DNA at map coordinate 0/1.0 (the "true" *Eco*RI restriction site) and at map positions 0.25, 0.29, 0.33, 0.42, 0.49, and 0.93 as well as others which were not identified. Judging from the rapidity with which the 0.20 SV40 fractional length fragment is produced from the *Hpa*II endonuclease created linear DNA, map coordinate 0.93 seems to be the second most readily cleaved site by *Eco*RI-$Mn^{2+}$. The 0.42 and 0.33 sites are cleaved with about equal probability but more slowly than the 0.93 site. Of the less frequently cleaved sites 0.25, 0.29, and 0.49, the 0.25 site seems to be cleaved slowest under the conditions used.

(C) *Effect of Ionic Composition on the EcoRI-$Mn^{2+}$ Reaction.* Whereas there is appreciable cleavage of *Eco*RI endonuclease generated linear DNA by *Eco*RI-$Mn^{2+}$ in 100 mM Tris (pH 7.5), there is very little further cleavage of the full length linear DNAs with 200 mM Tris buffer (compare tracks a and b in Figure 9); only after extensive incubation was there substantial cleavage of the *Eco*RI endonuclease generated linear DNA at the higher Tris concentration. Addition of 50 mM $Na^+$ to the *Eco*RI-$Mn^{2+}$ reaction (with 100 mM Tris buffer) reduces the rate of cleavage at the pseudo-*Eco*RI restriction sites (compare tracks c and e with tracks b and d in Figure 9). The rate of cleavage at the pseudo-*Eco*RI restriction sites is noticeably increased in 10 mM Tris buffer, but, even with $Mg^{2+}$ as the only cation, pure *Eco*RI endonuclease yields smaller fragments from SV40 DNA (Polisky et al., 1975) under these conditions.

(D) *Effect of DNA-Binding Dyes on the EcoRI-$Mn^{2+}$ Reaction.* When ethidium bromide is added to the *Eco*RI-$Mn^{2+}$ reaction, there is a progressive inhibition of the cleavages at pseudo-*Eco*RI restriction sites until, with 50 $\mu$g of ethidium bromide per mL, only a single cleavage occurs (Figure 10). The remaining cleavage at high ethidium bromide levels occurs at the authentic *Eco*RI restriction site since the predominant

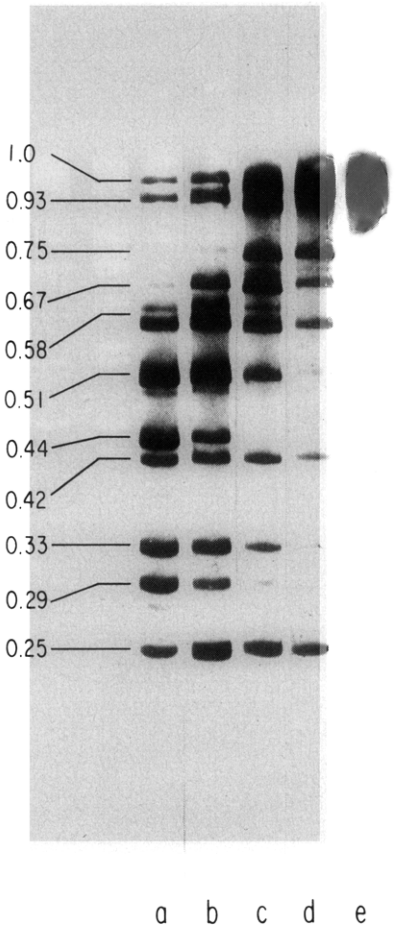


FIGURE 10: Effect of ethidium bromide on *Eco*RI endonuclease digestion of SV40 DNA in the presence of $Mn^{2+}$. SV40 (I) DNA (0.4 $\mu$g) was digested with 2 units of *Eco*RI endonuclease in 100 mM Tris (pH 7.5), 2 mM $Mn^{2+}$ and (a) 0, (b) 1, (c) 5, (d) 10, and (e) 50 $\mu$g/mL of ethidium bromide for 30 min at 37 °C.

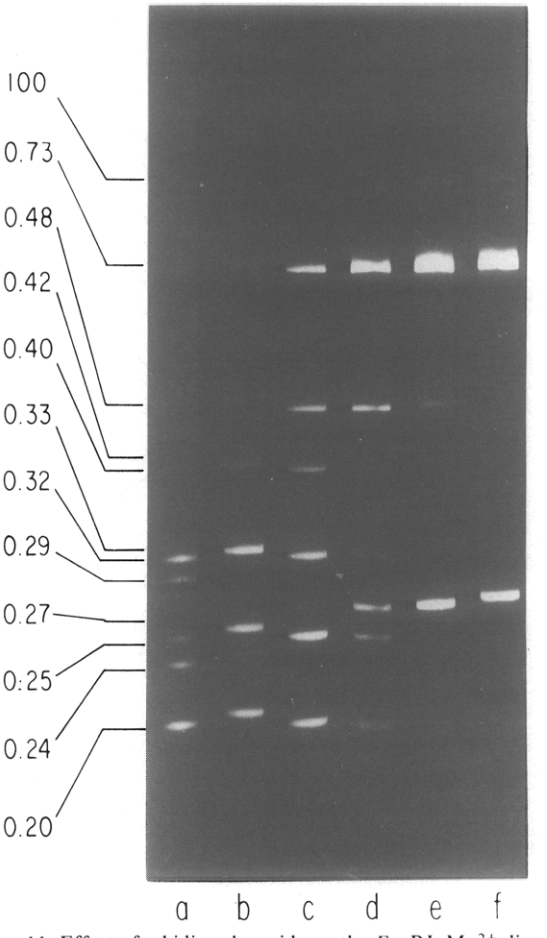


FIGURE 11: Effect of ethidium bromide on the *Eco*RI–$Mn^{2+}$ digestion of *Hpa*II endonuclease generated linear SV40 DNA. *Hpa*II endonuclease generated linear SV40 DNA (0.2 $\mu$g) was digested with about 2 units of *Eco*RI endonuclease in 100 mM Tris (pH 7.5), 2 mM $Mn^{2+}$ and (a) 0, (b) 1, (c) 5, (d) 10, (e) 20, and (f) 40 $\mu$g/mL of ethidium bromide for 30 min at 37 °C.

fragments produced by *Eco*RI endonuclease digestion of *Hpa*II endonuclease generated linear SV40 in the presence of high levels of ethidium bromide are 0.73 and 0.27 SV40 fractional length (Figure 11, tracks e and f). At intermediate levels of ethidium bromide, the *Eco*RI–$Mn^{2+}$-mediated cleavages are affected differentially. As the ethidium bromide concentration is increased, the 0.75 and 0.25 fractional length fragments disappear most slowly (Figure 10). That can be explained if cleavage of SV40 DNA at map position 0.25 was less affected by ethidium bromide than other "pseudo"-*Eco*RI restriction sites. The finding that 0.48 and 0.25 SV40 length fragments are among the last to disappear when *Hpa*II endonuclease generated linear DNA is digested in the presence of $Mn^{2+}$ and higher levels of ethidium bromide supports that view (Figure 11). Thus, binding of ethidium bromide to DNA eliminates the aberrant cleavages caused by *Eco*RI–$Mn^{2+}$ and the site which is cleaved most slowly with *Eco*RI–$Mn^{2+}$ is the least inhibited by ethidium bromide binding.

Other DNA-binding, intercalating dyes, for example, actinomycin D, methylene blue, acridine orange, and azure C, inhibit the *Eco*RI–$Mn^{2+}$ catalyzed cleavage at "pseudo-*Eco*RI" sites (data not shown). With actinomycin the inhibition is least at the 0.25 and 0.33 site as judged by the accumulation of the 0.75–0.25 and 0.67–0.33 fragment pairs. With the other dyes strong inhibition of cleavage at the 0.93 sites and relatively weak inhibition at the 0.25, 0.33, and 0.42 sites is reflected in the accumulation of 0.25, 0.33, and 0.58 length fragments and the disappearance of the 0.44 length fragment.

The pattern of inhibition by the nonintercalating dye, methyl green, is quite different. Cleavage at all but the true *Eco*RI restriction site is progressively inhibited by higher levels of methyl green but the 0.93 SV40 length fragment persists even at a methyl green concentration of 50 $\mu$g/mL suggesting that cleavage at the 0.93 site is least inhibited by methyl green. Persistence of the 0.71–0.29 and the 0.67–0.33 fragment pairs as well as the 0.60 (generated by cleavage at 0.33 and 0.93) and 0.58 (generated by cleavage at 0.42) fragments in the presence of 50 $\mu$g/mL of methyl green suggests that map positions 0.20 and 0.33 are less sensitive to inhibition than the 0.42 site.

(E) *Effect of $Mn^{2+}$ on the Specificity of Cleavages Catalyzed by HpaII and HindIII Endonucleases.* Various concentrations of $Mn^{2+}$ replacing $Mg^{2+}$ in *Hpa*II endonuclease reaction mixtures caused no change in the number of cleavages of SV40 DNA; under all conditions tested, full length linear DNA was the exclusive product. However, when $Mn^{2+}$ replaced $Mg^{2+}$ in the *Hin*dIII endonuclease reaction, there was extensive fragmentation of SV40 DNA (compare track b and track a in Figure 12) indicating that $Mn^{2+}$ also permits *Hin*dIII endonuclease to make additional cleavages. The map locations of these sites have not yet been determined.

## Discussion

Our findings, as well as those of Polisky et al. (1975), show

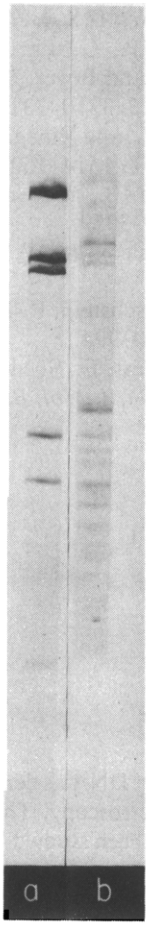


FIGURE 12: Effect of $Mn^{2+}$ on *Hin*dIII endonuclease digestion. *Hin*dIII endonuclease generated DNA fragments (0.1 μg) were further digested with 1 unit of *Hin*dIII endonuclease for 3 h at 37 °C in 10 mM Tris, pH 7.5, 50 mM NaCl, 0.5 mM dithiothreitol containing (a) 10 mM $Mg^{2+}$ and (b) 10 mM $Mn^{2+}$.

that the specificity attributed to *Eco*RI endonuclease is strongly dependent on the digestion conditions. Under standard conditions (100 mM Tris, pH 7.5, 2–10 mM $Mg^{2+}$) SV40 and λ phage DNA have 1 and 5 *Eco*RI endonuclease cleavage sites, respectively. But when $Mn^{2+}$ replaces $Mg^{2+}$ in the digestion reaction, both are almost pulverized; similarly, adenovirus type 2 DNA, which is cleaved five times by *Eco*RI endonuclease in the presence of $Mg^{2+}$ (Petterson et al., 1973), undergoes very extensive cleavage with $Mn^{2+}$ (data not shown). We consider two explanations for these observations: our *Eco*RI endonuclease preparation is contaminated with another endonuclease(s) that catalyzes these unexpected cleavages, or that the specificity of the *Eco*RI endonuclease, per se, varies depending upon the conditions (e.g., ionic strength, pH, divalent cation, etc.). The putative contaminating endonuclease(s), proposed in the first explanation, must be (a) inactive with $Mg^{2+}$; (b) site-specific, since a characteristic and transient pattern of fragments is produced; and (c) able to create cohesive ends that permit efficient cyclization of the fragments to occur. A relevant, but not conclusive, argument against the first explanation is the fact that several different purified preparations of *Eco*RI endonuclease also produce the same additional cleavages in SV40 and λ DNA with $Mn^{2+}$. Overall, we regard the existence of a contaminating endonuclease as far less likely than the $Mn^{2+}$-induced modified specificity model.

How does $Mn^{2+}$ alter the specificity of *Eco*RI endonuclease cleavage of DNA? Relevant to this question is the nature of the nucleotide sequences at which the novel cleavages occur. *Eco*RI endonuclease, under standard condition, cleaves DNA at the symmetric hexanucleotide sequence GAATTC (Hedgepeth et al., 1972). We regard the possibility, suggested by Polisky et al. (1975), that $Mn^{2+}$ permits *Eco*RI endonuclease to cleave DNA at AATT sequences regardless of what nucleotides are located at their 5′ or 3′ ends, as most plausible. If cleavages can occur at AATT sequences having any one of the four nucleotides at their 5′ and 3′ ends, the frequency, assuming a random arrangement of the four nucleotides, would be on the average once in 256 nucleotides rather than 4096 nucleotides, or an increase of 16 times. The variation in the rate of cleavage at pseudo-*Eco*RI restriction sites could result from the type of substitutions surrounding the AATT sequence. For example, a sequence with only the 5′-G changed might be cleaved more readily than one in which both the 5′-G and 3′-C were substituted; or, a sequence in which A replaces the 5′-G may be cleaved more rapidly than one in which a pyrimidine occurs at that position. These predictions will be testable as the sequence of SV40 DNA becomes available; for the present it is of interest that the sequence GAATTT occurs at map position 0.42 (Volckaert et al., 1977).

Amongst the divalent metal ions we have tested with *Eco*RI endonuclease, $Mn^{2+}$ is unique in changing its specificity. $Cu^{2+}$ and $Ca^{2+}$ ions inhibit the enzyme while $Zn^{2+}$ has no apparent effect. It is interesting to note that $Mn^{2+}$ ion also changes the specificity of other enzymes related to nucleic acids such as *E. coli* RNA polymerase (Paddock et al., 1974), *E. coli* DNA polymerase I (Berg et al., 1963), and DNase I (Melgar and Goldthwait, 1968).

Thus far only the restriction specificity of *Eco*RI and *Hin*dIII endonucleases have been altered in the presence of $Mn^{2+}$, but a systematic reexamination of the cleavage patterns of many more restriction endonucleases in the presence of $Mn^{2+}$ should be done. It would also be interesting to test whether the specificity of methylation by the *Eco*RI or *Hin*dIII methylases is also altered in the presence of $Mn^{2+}$.

Restriction endonucleases play a key role in a variety of nucleic acid studies; therefore, having greater control of the specificity of these enzymes by manipulating the reaction conditions facilitates these investigations. For example, molecules with no *Eco*RI restriction sites can still be cleaved to discrete fragments having cohesive ends if $Mn^{2+}$ is added to the reaction; deletions can be introduced into molecules having no functional *Eco*RI restriction site by partial digestion with *Eco*RI–$Mn^{2+}$ and rejoining of the remaining ends (Charney and Berg, unpublished results).

## Acknowledgment

We are grateful for the gift of *Eco*RI endonuclease from R. W. Davis, P. Modrich, and R. Roberts. We thank R. W. Davis for his advice and M. Thomas for her assistance.

## References

Arber, W. (1974), *Prog. Nucleic Acid Res. Mol. Biol. 14,* 1–37.

Berg, P., Fancher, H., and Chamberlin, M. (1963), *Inf. Macromol., Symp., 1962.*

Greene, P. J., Betlach, M. C., and Boyer, H. W. (1974), *Methods Mol. Biol. 7,* 87–110.

Hedgpeth, J., Goodman, H. M., and Boyer, H. W. (1972), *Proc. Natl. Acad. Sci. U.S.A. 69,* 3448–3452.

Hirt, B. (1967), *J. Mol. Biol. 26,* 365–369.

Melgar, E., and Goldthwait, D. A. (1968), *J. Biol. Chem. 243,*

4409-4416.
Mertz, J. E., and Davis, R. D. (1972), *Proc. Natl. Acad. Sci. U.S.A. 69*, 3370-3374.
Modrich, P., and Zabel, D. (1976), *J. Biol. Chem. 251*, 5866-5874.
Morrow, J. R., and Berg, P. (1973), *Proc. Natl. Acad. Sci. U.S.A. 69*, 3365-3369.
Mulder, C., and Delius, H. (1973), *Proc. Natl. Acad. Sci. U.S.A. 69*, 3215-3219.
Paddock, G. V., Heindell, H. C., and Salser, W. (1974), *Proc. Natl. Acad. Sci. U.S.A. 71*, 5017-5021.
Parker, R. C., Watson, R. M., and Vinograd, J. (1977), *Proc. Natl. Acad. Sci. U.S.A. 74*, 851-855.
Petterson, U., Mulder, C., Delius, H., and Sharp, P. A. (1973), *Proc. Natl. Acad. Sci. U.S.A. 70*, 200-204.
Polisky, B., Greene, P., Garfin, E. E., McCarthy, B. J., Goodman, W. M., and Boyer, H. W. (1975), *Proc. Natl. Acad. Sci. U.S.A. 72*, 3310-3314.
Radloff, R., Bauer, W., and Vinograd, J. (1967), *Proc. Natl. Acad. Sci. U.S.A. 57*, 1514-1521.
Sharp, P. A., Sugden, B., and Sambrook, J. (1973), *Biochemistry 12*, 3055-3059.
Smith, H. O., and Wilcox, K. W. (1970), *J. Mol. Biol. 51*, 379-391.
Takemoto, K. K., Kirschstein, R. L., and Habel, K. (1966), *J. Bacteriol. 92*, 990-994.
Volckaert, G., Contreras, E., Soeda, A., Van de Voorde, A., and Fiers, W. (1977), *J. Mol. Biol. 110*, 467-510.

# Inhibition of *Escherichia coli* RNA Polymerase by Bis(1-anilino-8-naphthalenesulfonate)†

Felicia Ying-Hsiueh Wu and Cheng-Wen Wu*,‡

ABSTRACT: Bis(1-anilino-8-naphthalenesulfonate) [bis(Ans)] is a dimer of 1-anilino-8-naphthalenesulfonate with a C-C linkage at the 4,4′ positions of the naphthalene rings. More than 90% of RNA polymerase activity is inhibited by $10^{-5}$ M bis(Ans), while no inhibition is observed with Ans at the same concentration. The concentration of bis(Ans) required for 50% inhibition is about $4 \times 10^{-6}$ M using various DNA templates. The inhibition can be partially prevented by preincubation of the enzyme with DNA and/or nucleoside triphosphates. At $10^{-5}$ M, bis(Ans) has no effect on the binding of RNA polymerase to DNA as measured by retention of the enzyme-DNA complex on a nitrocellulose filter. However, little DNA retention was detected with $10^{-4}$ M bis(Ans). Kinetic studies and the differential effects of bis(Ans) on $^3$H-labeled vs. $\gamma$-$^{32}$P-labeled nucleotide incorporations into the RNA product indicate that bis(Ans) at concentrations of $\leq 10^{-5}$ M selectively inhibits RNA chain initiation. Using T7 DNA as template, we have found that bis(Ans) inhibits the synthesis of the dinucleotide pppGpC catalyzed by RNA polymerase. Bis(Ans) binds to enzyme but not DNA as demonstrated by gel filtration and fluorescence spectroscopy. The binding of bis(Ans) to RNA polymerase has been studied by a fluorimetric titration technique. The binding isotherms show multiple binding sites of the dye, which can be divided into two distinct classes: a class of 16-18 strong binding sites with apparent $K_d = 2 \times 10^{-6}$ M and a class of 34-36 weak binding sites with apparent $K_d = 2 \times 10^{-5}$ M. Glycerol-gradient centrifugation analysis has revealed that RNA polymerase dimerizes in the presence of $1 \times 10^{-4}$ M bis(Ans) but remains as a monomer at $1 \times 10^{-5}$ M bis(Ans) in the high-salt (0.5 M KCl) buffer. Both the fluorescence and sedimentation results indicate that binding of bis(Ans) to the strong sites on enzyme inhibits RNA chain initiation, whereas binding to the weak sites induces dimerization of the enzyme concomitant with loss of its ability to bind DNA template. Further fluorescence studies show that aromatic amino acid residues are involved in the binding of dye.

The process of DNA-dependent RNA synthesis is rather complex and can be divided into several successive steps (Goldthwait et al., 1970): (a) association, the binding of RNA polymerase to the DNA template; (b) initiation, the binding of NTPs[1] to the enzyme-DNA complex followed by the formation of the first phosphodiester bond; (c) elongation, the subsequent addition of NTPs to form a polyribonucleotide chain; and (d) termination, the cessation of chain growth with the release of RNA product from the enzyme and DNA. Several antibiotics and dyes have been shown to inhibit specifically one or more of these steps by complexing with RNA polymerase. For instance, it has been proposed that rifampicin inhibits initiation (Hartmann et al., 1967; Wehrli et al., 1968; di Mauro et al., 1969), although it allows the continued synthesis of dinucleoside tetraphosphate by RNA polymerase (Johnston and McClure, 1976). On the other hand, streptolydigin affects both initiation and elongation (Siddhikal et al., 1969; Schleif, 1969). We have reported earlier that Rose Bengal preferentially inhibits RNA chain elongation (Wu and Wu, 1973), while Congo red (Krakow and von der Helm, 1970) and gallin (Liao et al., 1974) were found to block binding of RNA polymerase to DNA. All these inhibitors are important tools for elucidating the molecular mechanism of gene transcription.

† From the Department of Biophysics, Albert Einstein College of Medicine, New York, New York 10461. *Received July 6, 1977.* This work was supported in part by research grants from the National Institutes of Health (GM 19062) and the American Cancer Society (BC-94C).

‡ Research Career Development Awardee of the National Institutes of Health and a recipient of the Irma T. Hirschl Scientific Career Award.

[1] Abbreviations used are: NTP, nucleoside triphosphate; Ans, 1-anilino-8-naphthalenesulfonate; bis(Ans), bis(1-anilino-8-naphthalenesulfonate); EDTA, ethylenediaminetetraacetic acid; WASP solvent, $H_2O$-saturated $(NH_4)_2SO_4$ (pH 8)-2-propanol in volume ratios of 18:80:2, respectively.

0006-2960/78/0417-0138$01.00/0 